MARS-ANALOG RADAR INVESTIGATION OF TEPHRA AND BURIED ICE IN THE VALLEY OF TEN THOUSAND SMOKES, KATMAI NATIONAL PARK, ALASKA. D. M. H. Baker[1], P. L. Whelley[1,2], J. A. Richardson[1], A. Matiella Novak[3]. [1]NASA Goddard Space Flight Center, Greenbelt, MD (david.m.hollibaughbaker@nasa.gov), [2]University of Maryland, College Park, MD, [3]Johns Hopkins University Applied Physics Laboratory, Laurel, MD.

Introduction: The detection and characterization of off-polar subsurface ice on Mars is important for a variety of science and human exploration objectives [1,2]. Radar techniques, including orbital synthetic aperture radar (SAR) and surface-deployed ground-penetrating radar (GPR), are key to achieving these objectives. In particular, polarimetric SAR backscattering characteristics have been used to evaluate the presence of surface and subsurface ice on planetary bodies [see 3] and will be critical measurements to be obtained by future mission to Mars (e.g., International Mars Ice Mapper [2]).

Here, we test radar techniques for subsurface ice detection and characterization at a martian analog site in the Valley of Ten Thousand Smokes (VTTS) in Katmai National Park, Alaska. This site provides an excellent laboratory for understanding the origin and evolution of thick tephra deposits and interactions with water and water ice on planetary bodies. We conducted analyses of radar data collected over buried glacial ice and other volcanic units within the VTTS to explore the units' physical properties that affect the radar response.

Field Site: The VTTS is located on the Alaskan peninsula along an active arc of Quaternary volcanoes. The 1912 eruption at Novarupta produced 11 km^3 of ignimbrites and 17 km^3 of fall deposits (rhyolitic to andesitic) that filled the valley and thickly buried (up to ~10 m) and insulated glacial ice of the Knife Creek Glaciers (Fig. 1) [4]. Vegetation is sparse throughout the valley due to the tephra and aeolian activity. The unique stratigraphic relationship between the thick, low-density tephra and glacial ice is analogous to mid-latitude areas on Mars where dust and remobilized material has accumulated on top of glaciers and extensive ice sheets.

Methodology: *SAR.* We used UAVSAR airborne polarimetric SAR data (1.26 GHz) collected in June 2017 (katmai_28020_17065_095_170616 _L090_CX_01, 5x6 m/pixel) to assess radar scattering behavior within the top few meters of the surface (Fig. 1). Ground-projected complex cross product data were used to calculate the degree of linear polarization (m_l) (sensitive to near-surface layering) and Circular Polarization Ratio (CPR) [e.g., 5,6], which is a common product for assessing ice and roughness characteristics [3]. In contrast to conventional calculations [3], we normalized m_l and *CPR* to the average polarized intensity to limit added noise from the unpolarized component [Ref. 6, Eqs. 13 and 14]. L-band SAR penetration depth (δ) is approximately 0.85 to 4.2 m, estimated as $\delta = \lambda/2\pi\ (\sqrt{\varepsilon'/\varepsilon''})$, where $\lambda = 0.238$ m, $\varepsilon' = 5.0$ (real dielectric) and $\varepsilon'' = 0.02$ (low loss, dry) to 0.1 (higher loss, moist) (imaginary part of dielectric).

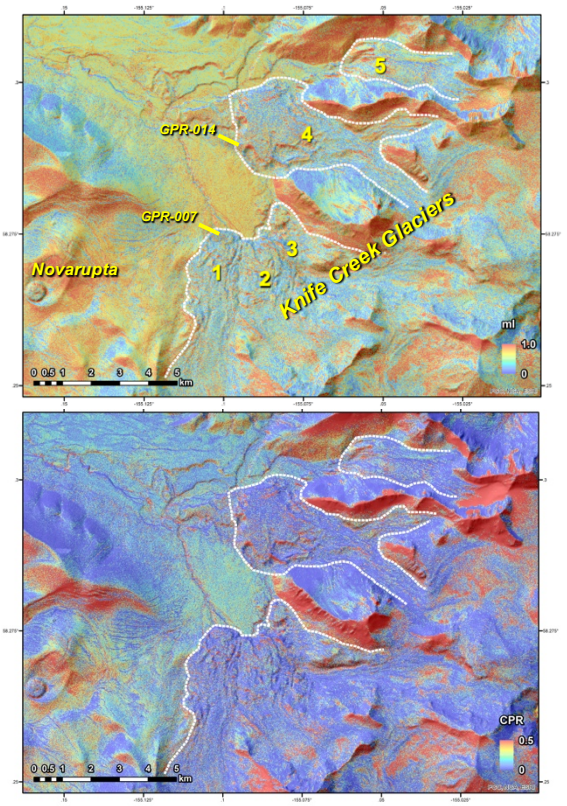

Fig. 1. Upper VTTS showing UAVSAR data with degree of linear polarization (top) and circular polarization ratio (bottom). Labeled and outlined are Knife Creek Glaciers 1-5 and GPR sites at the glacier termini.

GPR. Field observations in June 2022 included GSSI GPR surveys (400 MHz) completed over accessible portions of the termini of Glaciers 1 and 4 (Fig. 1) and proximal, ice-free fall deposits. Standard processing was applied to GPR radargrams for interpretation.

Trenches and Permittivity. Coordinated trenches and soil moisture/dielectric permittivity measurements were completed using a Stevens HydaGO probe. Probe measurements were collected at the surface every 5 m along the GPR lines and at depth every 10 cm in trenches.

Results and Interpretations: *SAR.* The glaciers show generally high total SAR backscatter compared to the surrounding plains, likely owing to its hummocky ablation- and flow-related surface topography. Excluding steep surface slopes, values for the degree of linear polarization on the glaciers are low to moderate, and CPR values are very low (<<0.5) (Fig. 1). This is in contrast to

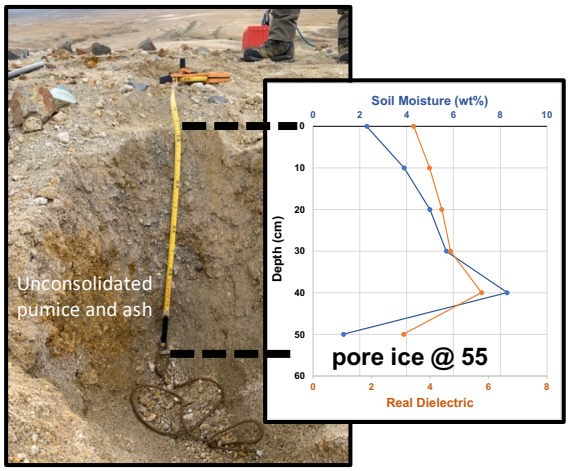

Fig. 2. (Left) Trench along GPR line -014 at Glacier 4. (Right) Soil moisture probe measurements with depth in trench.

the observation of very high CPR values for ice deposits elsewhere in the solar system [3]. The surrounding plains exhibit moderate to high values consistent with observed abundant near-surface layering and surface rocks approaching the radar wavelength.

Subsurface Stratigraphy. Trenches and probe measurements (Fig 2) revealed relatively dry overburden (pumice and ash), transitioning to pore ice at 40-50 cm depths and glacial ice starting at depths of ~1-2 m that varied spatially. The top ~0.5 m had real dielectric values of ~3-5 (Fig. 2), within range of values expected for martian regolith. Corresponding soil moisture measurements ranged from ~2-8 wt% (Fig. 2).

The relatively dry and low-density nature of the tephra overburden and low-loss glacial ice allowed excellent penetration of the GPR signal down to 10 m or greater (Fig. 3). Laterally continuous reflectors at ~50 cm and 1 m depths at Glacier 4 correlate with transitions from dry tephra to pore ice and pore ice to glacial ice, respectively. Reflectors within the tephra are likely due to variations in moisture conditions, grain size, and density. Within the glacial ice, numerous reflectors and hyperbolas are associated with bands of entrained sediment and fractures.

Discussion and Implications: The physical properties of the tephra and glacial ice allow for excellent transmission of airborne SAR L-band signals under the observed dry conditions in June 2022. However, the very low CPR values in the June 2017 SAR observations suggest that the physical properties of either the overburden or ice are not ideal for generating double-bounce signatures or a coherent backscatter opposition effect indicative of subsurface ice. Possible explanations include wet conditions at the time of SAR observation (thus attenuating the radar signal), thicker (>>1m) tephra over much of the glacier, and/or lack of appropriately spaced and sized scatters within the ice. Additional field observations of tephra and ice over more regions of the glaciers and coordinated SAR observations would help to elucidate these factors. In turn, these observations will help to determine the major factors that may cause variability in radar response to buried ice on Mars.

In addition, these glaciers are an end-member analog to debris-covered ice on Mars. As in VTTS, fine-grained deposits and lags of sediment have helped to preserve ice in the mid-latitudes of Mars and may exhibit variable ice concentration with depth. Many debris-covered glaciers on Earth show sharp transitions at depth between glacial ice and rock-fall dominated supraglacial debris with high porosity. In contrast, the finer-grained, thick tephra on glaciers in the VTTS results in a more gradual transition, including a zone of pore-filling ice between ice-free sediment and massive glacial ice at depth. GPR reflectors associated with these transitions in ice concentration showcase the ability of future sounding radars to map variations in subsurface ice concentrations at Mars.

Acknowledgments: We acknowledge support from the NASA Goddard Instrument Field Team (GIFT), permission from the National Park Service, Katmai National Park, and the University of Alaska International Volcanological Field School, led by Dr. Pavel Izbekov. UAVSAR data accessed from the Alaska Satellite Facility (ASF).

References: [1] MEPAG ICE-SAG Final Report (2019) http://mepag.nasa.gov/reports.cfm. [2] I-MIM Measurement Definition Team Final Report (2022) https://science.nasa.gov/researchers/ice-mapper-measurement-definition-team. [3] Carter, L.M. et al. (2011) Proc. IEEE, 99(5), 770–782. [4] Hildreth, W, and J. Fierstein (2012) *USGS Prof. Paper 1791*, 259 p. [5] Neish, C.D. et al. (2017) *Icarus* 281, 73–89. [6] Raney, K. et al. (2021) *Can. J. Rem. Sens.*, 47(1), 1–16.

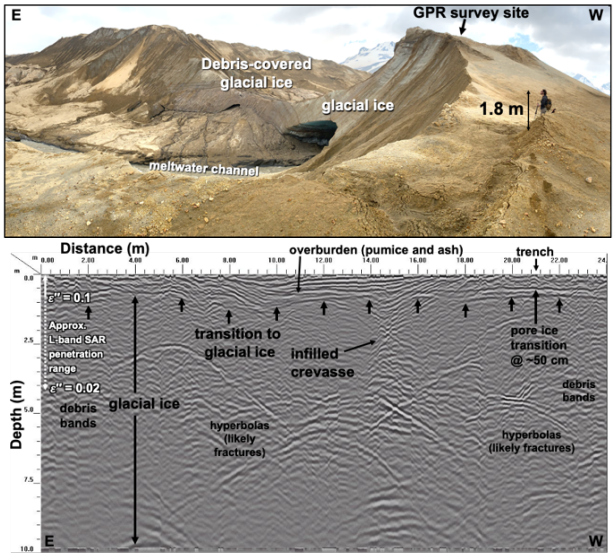

Fig. 3. (Top) Terminus of tephra-covered Glacier 4 at GPR site -014. (Bottom) GPR radargram (24-m long) taken on glacier surface, showing reflectors within tephra overburden and glacier ice at depth. Depth-corrected assuming $\varepsilon' = 5.0$. Approx. SAR penetration shown as white arrows in upper left.